Entangled Granular Media

Nick Gravish,[1] Scott V. Franklin,[2] David L. Hu,[3] and Daniel I. Goldman[1,*]

[1]School of Physics, Georgia Institute of Technology, Atlanta, Georgia 30332, USA
[2]Department of Physics, Rochester Institute of Technology, Rochester, New York 14623, USA
[3]School of Mechanical Engineering, Georgia Institute of Technology, Atlanta, Georgia 30332, USA

(Received 8 December 2011; published 17 May 2012)

We study the geometrically induced cohesion of ensembles of granular "u particles" that mechanically entangle through particle interpenetration. We vary the length-to-width ratio l/w of the u particles and form them into freestanding vertical columns. In a laboratory experiment, we monitor the response of the columns to sinusoidal vibration (with peak acceleration Γ). Column collapse occurs in a characteristic time τ which follows the relation $\tau \propto \exp(\Gamma/\Delta)$. Δ resembles an activation energy and is maximal at intermediate l/w. A simulation reveals that optimal strength results from competition between packing and entanglement.

DOI: 10.1103/PhysRevLett.108.208001 PACS numbers: 45.70.−n, 83.80.Fg

Many living and nonliving materials are composed of ensembles of nonspherical particles. In the biological world, ant rafts [1] and eagles nests [2] are held together through the interpenetration of body parts and branches, respectively. In soft condensed matter systems composed of ensembles of particles, particle shape influences rheological and structural properties like viscosity [3], yield stress [3,4], and packing density [5,6].

In studies of granular materials (GM), collections of athermal particles that interact through dissipative repulsive contact forces, most attention has been devoted to approximately spherical (convex) particle shapes [6–8]. Dry nonconvex granular particles also interact through repulsive contact forces. However, nonconvex particles possess the ability to interpenetrate, and thus, depending on the shape, may experience an effective cohesion through interpenetration. We refer to such interpenetrating ensembles as "entangled" ensembles. While the static packing of granular nonconvex particles [7,8] and the rheology of nonconvex particle suspensions [3] have been previously studied, the role of particle entanglement in granular dynamics and stability is unexplored.

In this Letter, we report on a laboratory experiment, computer simulation, and theory to elucidate the role of particle shape in the packing and stability of a model nonconvex granular system of u-shaped particles ("u particles"). Nonconvex particles in the shape of a u are one of the simplest shapes in which concavity can be systematically controlled by varying arm length. Similar to previous studies [9–12] of dry GM, we use vertical vibration to probe relaxation and rearrangement of the u-particle ensembles, thereby characterizing the effective cohesiveness of the entangled ensembles. We show that nonconvex particle shape leads to effects which are qualitatively different from concave dry GM and display phenomena similar to those observed in studies of wet cohesive granular materials [11].

Methods.—The u particles in our experiments consisted of steel staples (Duo-fast; Vernon Hills, Il.) of constant width, $w = 1.17$ cm, and variable length, l ($l/w \in [0.02, 1.125]$); see Figs. 1 and 2. The cross section of all particles was rectangular with a thickness of 0.5 mm and a width, 1.27 mm, which corresponded to a rod-like aspect ratio for $l/w = 0.02$ particles of approximately 14. Particles with $l/w = 0.02 \pm 0.02$, 0.13 ± 0.02, 0.15 ± 0.03, and 0.28 ± 0.04 were cut to length by hand and the remaining sizes were purchased. Columns occupied a volume $V = \pi h(d/2)^2$, and the bulk volume fraction was calculated as $\phi = \frac{M}{\rho_{st} V}$ where M is total particle mass and $\rho_{st} = 7.85$ g/cm^3 is the density of steel.

Sinusoidal vibration at a frequency of $f = 30$ Hz was generated by an electromagnetic shaker [VTS; Aurora, OH; Fig. 1(a)]. The shaker was controlled by LabVIEW and a Tecron 7550 power amplifier. Acceleration of the vibration table was measured by an accelerometer (PCB Piezotronics; Depew, New York). Columns were subjected to vibration for a maximum of 20 min (36 000 oscillation periods) or until complete column collapse occurred.

Column collapse was monitored using a digital camera (Point-Grey; Richmond, BC, Canada). Image capture was triggered at a constant phase in oscillation. Images were analyzed in MATLAB.

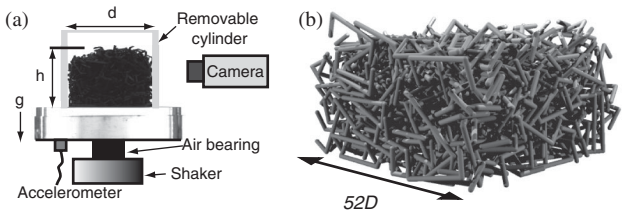

FIG. 1. Experiment and simulation of u-particle ensembles. (a) Freestanding vertical columns are formed on a vibration table and the collapse dynamics are observed under vertical vibration. (b) Computer generated ensembles of u particles.

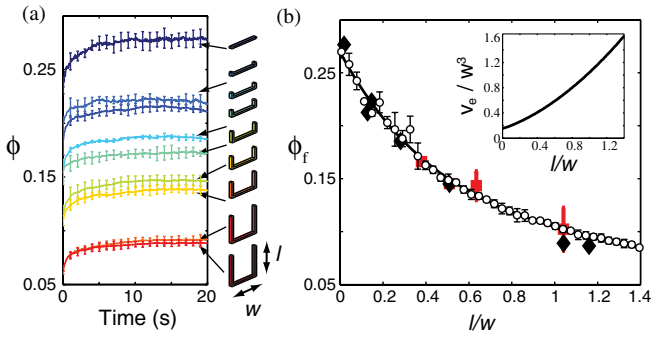

FIG. 2 (color online). Packing of u particles. (a) $\phi(t)$ during column formation. (b) Final packing fraction, ϕ_f, as a function of particle geometry in the experiment (column diameter $d = 4.4$ cm diamonds and $d = 5.6$ cm squares) and simulation (white circles). The line is the theoretical prediction from the random contact model. (Inset) Excluded volume of sphero-cylinder u particles from the simulation.

In the Monte Carlo simulation [Fig. 1(b)], we studied the packing of ensembles of u particles. U particles were created from three sphero-cylinders, each of diameter D, placed at right angles with backbone width $W = 14D$, measured from center to center of arms, and variable barb length $l/w \in [0, 1.3]$. We estimate the particle volume to be $v_p = \pi(D/2)^2[2L + w + \frac{4}{3}(D/2)]$ The cross-sectional particle shape differed between simulation and experiment (rectangular in experiment, circular with diameter D in simulation). The excluded volume, v_e, was numerically estimated by determining the probability p of overlap between two randomly oriented and positioned particles within a fixed spherical volume V. Overlap was determined by computing the minimum distance between all line segments composing the two particles; if this distance was less than the sphero-cylinder diameter D, particles overlapped. The excluded volume is the product of overlap probability and the sphere volume $v_e = pV$.

We used a packing algorithm to generate packings of nonoverlapping u particles. Packing proceeded in two steps: First, particles were placed at random positions and orientations inside a cubic volume of the cross-sectional area $(52D \times 52D)$. If particle placement resulted in overlap, the placement was rejected and a new position was randomly selected. If, after 10 000 iterations, a nonoverlapping particle location was not found, the algorithm proceeded to step two. In the second step, randomly selected particles were displaced downwards a small random direction and distance $\frac{D}{10}$. If the new location of the particle resulted in particle overlap, the particle was returned to the original location and a new particle chosen. The algorithm was halted after the center of mass height of the ensemble reached a steady state. ϕ_f of the simulated packing was determined by measuring the average height of the pile to obtain the occupied volume and then dividing this by the total volume of particles.

Column formation.—In the experiment, collections of particles with fixed l/w were formed into freestanding cylindrical columns with column diameter, $d = 4.4$ cm, and height, $h_0 = 3$ cm. Columns were prepared by pouring particles into a cylindrical container followed by a sinusoidal vibration of the base for 600 oscillation periods at a frequency of 30 Hz, and peak acceleration, $\Gamma = 2$ (in units of gravitational acceleration g). We confirmed that the steady-state volume fraction was reached through our preparation protocol in separate experiments conducted over 1800 oscillation periods.

The final volume fraction of the column following packing, ϕ_f, was a monotonically decreasing function of l/w [Fig. 2(b)]. The value of ϕ_f observed for $l/w = 0.02$ particles was within the range observed in cylindrical rod experiments with a comparable aspect ratio (length/thickness ≈ 14) that packs to $\phi_f = 0.28$–0.34 depending upon preparation [6,8,13].

Following the packing preparation, we removed the confining container, leaving the column freestanding [Fig. 3(a)]. During the removal of the confining cylinder, the $l/w = 0.02$ particles were marginally stable with a partial column collapse occurring approximately 50% of the time, similar to the results reported in [6]. Spontaneous collapse of the $l/w > 0.02$ columns was rarely observed.

Column collapse.—We applied sinusoidal vibration of frequency $f = 30$ Hz to the base of the freestanding column and observed the collapse process (see Supplemental Material [14]). We characterized collapse dynamics by monitoring the centroid height, $h(t)$, of the column (Fig. 3). The collapse duration decreased with increasing Γ [Fig. 3(b)] and collapse dynamics were well described by a stretched exponential fit function $\frac{h(t)}{h_0} = e^{[-(\frac{t}{\tau})^\beta]}$. The parameter τ is the characteristic collapse time and β is the stretching parameter [15]. The stretched exponential function is frequently applied to the description of relaxation dynamics of disordered systems [15].

Consistent with previous studies [10,16], β was in the range of 0.5–1 and decreased slightly as Γ increased but was independent of particle geometry. For fixed l/w, τ decreased with increasing Γ. The logarithm of τ increased

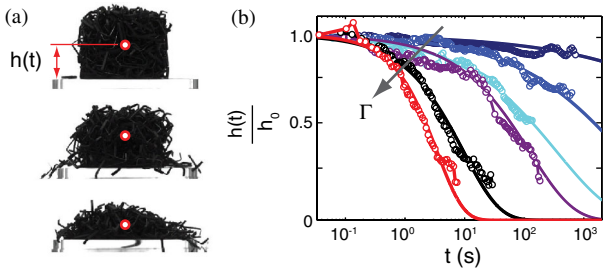

FIG. 3 (color online). Collapse dynamics. (a) The normalized centroid height, $h(t)/h_0$ (red dot) of the column during collapse. Vibration parameters are $\Gamma = 2$, $f = 30$ Hz, and images are separated by 90 oscillation periods. (b) Relaxation of $h(t)/h_0$ is shown for $l/w = 0.379$ for $\Gamma = 1.23, 1.48, 1.70, 1.96, 2.20, 2.53$, respectively. Fit lines are stretched exponentials given in the text.

with $1/\Gamma$ [Fig. 4(a)] and was fit by an exponential $\tau = f^{-1}e^{\Delta/\Gamma}$ with Δ as the single fit parameter and $f = 30\,\mathrm{Hz}$.

The exponential fit is indicative of an Arrhenius-like process observed in the relaxation of activated systems. The Arrhenius process describes the escape probability of a thermally or mechanically activated particle from a potential well of depth Δ. In thermal systems, the escape time is proportional to one over the Boltzmann factor $\exp(-\frac{E}{kT})$, where E is the activation energy required to overcome the potential barrier. In our system, thermal effects are negligible, and we hypothesize that the mechanical excitation plays the role of a thermal energy source (Γ analogous to kT) and Δ is analogous to an energy barrier resulting from particle entanglement.

Column collapse occurred through the separation of entangled particles during vibration. We therefore expected that the hindrance of motion due to particle entanglement—and thus Δ—would increase monotonically with the size of the concave region and thus particle length. Instead we found that Δ was a nonmonotonic function of l/w [Fig. 4(b)] with Δ reaching a maximum value at intermediate $l/w = 0.394 \pm 0.045$ [17]. Δ appears in an exponential and thus the relaxation time for fixed Γ displays a surprising sensitivity to the variation of particle shape [inset, Fig. 4(b)]. We posit that the maximum in Δ is related to the statistics of particle entanglement within the bulk, and we study entanglement propensity in a theoretical model and simulation.

Model and simulation.—In simulation we generated u-particle ensembles of varying l/w [Fig. 1(b)] and measured the packing fraction, ϕ_f. We found excellent agreement between experiment and simulation in ϕ_f [Fig. 2(b)]. The scaling of ϕ_f with l/w can be understood through the random contact model originally developed to describe the packing of hard rods [8].

Assuming a homogeneous packing of particles, the random contact model relates the excluded volume, v_e, occupied volume, v_p, and average number of particle contacts, C, to the bulk packing fraction ϕ_f through $\phi_f = C\frac{v_p}{v_e}$.

We numerically computed v_e [Inset Fig. 2(b)] and found excellent agreement between the prediction of the random contact model and the values of ϕ_f measured in experiment and simulation [Fig. 2(b)]. Fitting the random contact model to experimental and simulation packing data we obtained $C = 8.74 \pm 0.04$, close to the value found in studies of colloid and granular rod packing [6,8,13].

We hypothesized that particle entanglement within the column would influence the relaxation time during vertical vibration. Thus, we expected that the maximum in Δ should correspond to a maximum in the density of particle entanglements. In simulation, we defined two particles as entangled when the center line of one particle intersected the internal plane of the neighboring particle [Inset Fig. 5(a)]. We measured the number of entanglements per particle N for each particle in simulation. The probability distribution function, $P(N)$, was sensitive to l/w [Fig. 5(a)] with mean value $\langle N\rangle$ increasing monotonically with l/w [Fig. 5(b)]. The increase was sublinear indicating that $\langle N\rangle$ grew slower than that of the particle's concave area $(l - D)(w - 2D)$.

The scaling of $\langle N\rangle$ with l/w can be determined by considering the solid volume occupied by the entangled particles in the focal particle's concave region (the concave area with infinitesimal thickness δ). Assuming a

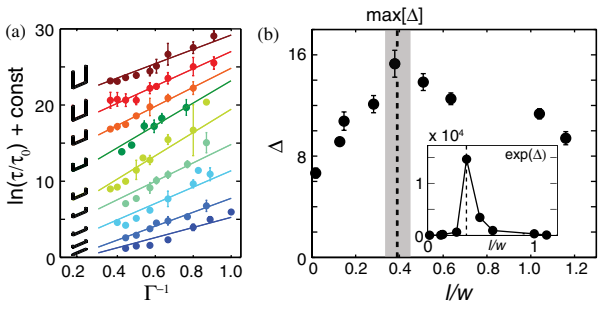

FIG. 4 (color online). Particle shape and optimal geometric cohesion. (a) The logarithm of the relaxation time versus inverse acceleration with exponential fit lines $\tau = f^{-1}e^{\Delta/\Gamma}$ ($\tau_0 = 1$ s, $f = 30\,\mathrm{Hz}$). Curves are offset vertically by an arbitrary constant for clarity. Error bars are standard deviation of 4 or greater replicates. (b) Δ as a function of l/w. Dashed line indicates estimated maximum of Δ (see [17]). Error bars represent 95% confidence interval of the best fit lines from (a).

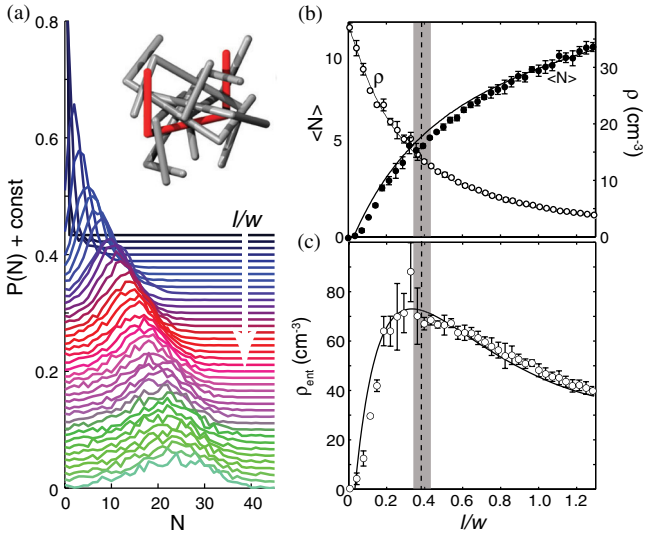

FIG. 5 (color online). Statistics of particle entanglement in simulation. (a) The probability distribution of the entanglement number N as a function of l/w. Curves are shifted vertically for clarity; $l/w = 0$ at the top and increases in increments of 0.036 down. Inset: A particle (colored red) containing 6 entangled neighbors. (b) Mean values for N and ρ measured in simulation (circles) and the theoretical fit (black line). (c) Density of entanglements as a function of l/w and the theoretical fit (black line). The vertical dashed line and gray bar correspond to the mean and standard deviation of the estimated maximum of Δ from the experiment, respectively.

homogeneous packing, the solid volume in this region is $V_{\text{ent}} = \phi_f(l-D)(w-2D)\delta$. Since each entangled particle contributes only a portion to V_{ent} in the shape of an ellipse of thickness δ, on average $V_{\text{ent}} = \alpha\langle N\rangle\pi\delta\frac{D^2}{4}$, where $\alpha > 1$ accounts for the nonplanar crossings [Inset Fig. 5(a)]. Solving the above relations yields $\langle N\rangle = \frac{4C}{\pi\alpha}(\frac{v_p(l-D)(w-2D)}{v_e D^2})$. With a single fit parameter, $\alpha = 2.648 \pm 0.108$, we find excellent agreement between the predicted number of entanglements per particle and those measured in simulation [Fig. 5(b)].

The spatial density of particle entanglements is $\rho_{\text{ent}} = \langle N\rangle\rho$ where $\rho = \frac{C}{v_e}$ is the number density of particles [Fig. 5(b)]. Substitution for $\langle N\rangle$ yields $\rho_{\text{ent}} = \frac{4C^2}{\pi\alpha}(\frac{v_p(l-D)(w-2D)}{v_e^2 D^2})$ and again the simulation and theory are in good agreement [Fig. 5(c)] using the previously determined fit parameters C and α. Furthermore, the experimental maximum $\max[\Delta]$ at $l/w = 0.394 \pm 0.045$ is close to the value obtained in the simulation and theory of $l/w = 0.340 \pm 0.015$ suggesting that the large relaxation times for the intermediate u-particle columns is due to the high density of mechanical entanglements.

Conclusion.—Similar to rodlike particles [6,8,13], columns formed from u particles are stabilized through the inhibition of particle rotation and translation among the entangled particles. The addition of the transverse ends that form concave u particles leads to mechanical entanglement and increases column stability. However, the increase in entanglement with increasing length is offset by the decrease in particle packing density. These two trends conspire to generate a maximum in the density of mechanical entanglements in collections of nonconvex particles of intermediate l/w—thus, columns of these particles most strongly resist separation.

The random contact model utilized to explain the optimum geometry for entanglement of u-shaped particles assumes only uncorrelated particle contacts within the bulk. Thus, we expect the results to apply to rigid nonconvex particulate systems of all scales. For instance, a recent study of suspension rheology found that convex particles of differing shapes collapsed to a viscosity-stress master curve while concave particle did not collapse to this curve; this difference was attributed to particle entanglement effects [3]. At the microscale, polymers with rigid pendants oriented perpendicular to the polymer chain increase the internal molecular-free volume and hinder polymer motion, which significantly affects rheology similar to geometric entanglement [18]. At the macroscale, the strain-stiffening of model polymers is associated with entanglement [19]. Even organisms can benefit from geometric entanglement. For example the fire ant *Solenopsis invicta* and the army ant *Eciton burchelli* create waterproof rafts and shelters—which have been described as akin to living chain mail [20]—through the interlocking and entanglement of limbs and mandibles [1].

The authors would like to acknowledge Paul B. Umbanhowar for helpful discussions and Geoff Russell, Luis Saldana, and Nathan Jankovsky for help with the experimental fabrication. Funding support for N. G. and D. I. G. provided by NSF Physics of Living Systems No. 0957659. S. V. F. was supported by (NSF DMR-0706353). D. H. gratefully acknowledges the financial support of the NSF (PHY-0848894).

*daniel.goldman@physics.gatech.edu

[1] N. Mlot, C. Tovey, and D. Hu, Proc. Natl. Acad. Sci. U.S.A. **108**, 7669 (2011); C. Anderson, G. Theraulaz, and J. Deneubourg, Insectes Sociaux **49**, 99 (2002).
[2] M. Hansell, *Bird Nests and Construction Behaviour* (Cambridge University Press, Cambridge, 2000).
[3] E. Brown, H. Zhang, N. A. Forman, B. W. Maynor, D. E. Betts, J. M. DeSimone, and H. M. Jaeger, Phys. Rev. E **84**, 031408 (2011); C. Hsueh and W. Wei, J. Appl. Phys. **107**, 024905 (2010); R. Egres and N. Wagner, J. Rheol. **49**, 719 (2005).
[4] R. Kramb and C. Zukoski, J. Rheol. **55**, 1069 (2011).
[5] W. Man, A. Donev, F. H. Stillinger, M. T. Sullivan, W. B. Russel, D. Heeger, S. Inati, S. Torquato, and P. M. Chaikin, Phys. Rev. Lett. **94**, 198001 (2005).
[6] J. Blouwolff and S. Fraden, Europhys. Lett. **76**, 1095 (2006); K. Desmond and S. V. Franklin, Phys. Rev. E **73**, 031306 (2006); M. Trepanier and S. V. Franklin, *ibid.* **82**, 011308 (2010).
[7] A. Donev, I. Cisse, D. Sachs, E. Variano, F. H. Stillinger, R. Connelly, S. Torquato, and P. M. Chaikin, Science **303**, 990 (2004).
[8] A. Philipse, Langmuir **12**, 1127 (1996); Y. Jiao, F. H. Stillinger, and S. Torquato, Phys. Rev. E **79**, 041309 (2009).
[9] H. M. Jaeger, C. H. Liu, and S. R. Nagel, Phys. Rev. Lett. **62**, 40 (1989).
[10] P. Philippe and D. Bideau, Europhys. Lett. **60**, 677 (2002).
[11] S. Herminghaus, Adv. Phys. **54**, 221 (2005).
[12] I. Sanchez, F. Raynaud, J. Lanuza, B. Andreotti, E. Clement, and I. S. Aranson, Phys. Rev. E **76**, 060301 (2007); P. Richard, M. Nicodemi, R. Delannay, P. Ribiere, and D. Bideau, Nature Mater. **4**, 121 (2005).
[13] A. Wouterse, S. Luding, and A. Philipse, Granular Matter **11**, 169 (2009).
[14] See Supplemental Material at http://link.aps.org/supplemental/10.1103/PhysRevLett.108.208001 for a high speed video of column collapse.
[15] J. Phillips, Rep. Prog. Phys. **59**, 1133 (1996).
[16] J. Mattsson, H. Wyss, A. Fernandez-Nieves, K. Miyazaki, Z. Hu, D. Reichman, and D. Weitz, Nature (London) **462**, 83 (2009).
[17] We estimate the maximum of l/w in experiment using a weighted average of points near the peak.
[18] N. Tsui, A. Paraskos, L. Torun, T. Swager, and E. Thomas, Macromolecules **39**, 3350 (2006).
[19] E. Brown, A. Nasto, A. G. Athanassiadis, and H. M. Jaeger, Phys. Rev. Lett. **108**, 108302 (2012).
[20] M. Mitchell, *Complexity: A Guided Tour* (Oxford University Press, New York, 2009).